

Optical and Electrical Studies of 100 MeV $^{56}\text{Fe}^{7+}$ on Irradiated Indium phosphide

Rajendra Rathi¹, Sharad Tripathi²

¹Ramnarain Ruia Autonomous College, Department of Physics, Mumbai 400 019, India.

²G.N. Khalsa College (Autonomous), Department of Physics, Mumbai 400 019, India.

*Corresponding Author E-Mail: rajendrarathi@ruiacollege.edu

Abstract

Indium phosphide (InP) was irradiated with 100 MeV $^{56}\text{Fe}^{7+}$ ions for various ion fluences of 5×10^{12} , 5×10^{13} and $1 \times 10^{14} \text{ cm}^{-2}$ was studied for Optical and electrical parameters of the irradiated sample and comparison with the non-irradiated sample was accomplished. The changes in the optical parameters such as absorbance, energy band gap energy and defect density have been studied. Raman scattering spectroscopy measurements were carried out to understand disorders and related defects induced in the surface region of the crystalline indium phosphide due to the swift iron ion irradiation. The appearance of interference fringes with increasing amplitude and shift in the maxima and minima positions, in the Fourier transform reflectance spectra of irradiated samples showed the change in the refractive index of the irradiated layer due to presence of point defect or defect clusters in the sample. The changes in the electrical parameter such as barrier height, ideality factor and carrier concentration have been studied, using I-V and C-V measurements. Impact of increasing ion fluence was studied on energy band gap of irradiated sample.

Keywords: Swift iron ions; Indium phosphide; UV-IR, Raman scattering; FTIR

Introduction:

Indium phosphide (InP) is a direct band gap compound semiconductor widely used in optoelectronic and microwave devices (1). The properties of InP can be further transformed by swift heavy ion irradiation. Irradiation of InP with Au⁺, Pb⁺, Kr⁺ and Xe⁺ ions produced disorder region as well as large number of defects (2–4). Both disorder region and defects changed the properties of the irradiated samples. Under certain conditions, latent tracks in InP due to high electronic excitation have been observed. However, limited studies on the transition metal (i.e. Fe and Co) ion irradiation of InP have been reported (5-7). The size and density of nano structures were found to depend on the ion fluence (7). In the present work, the effects of 100 MeV $^{56}\text{Fe}^{7+}$ ion irradiation on InP for various ion fluences of 5×10^{12} , 5×10^{13} and $1 \times 10^{14} \text{ cm}^{-2}$ have been investigated by the Ultraviolet–visible spectroscopy, Raman scattering, Fourier transform infrared (FTIR) techniques. Schottky barrier diode on n-InP is fabricated by deposition of metal (Au) electrodes of 1 mm diameter on the implanted side and ohmic contact on the reverse side of the samples using the vacuum thin film deposition technique. Using Schottky barrier diode, the current – voltage (I-V) and the capacitance-voltage (C-V) measurements were carried out at room temperature.

Experimental:

Single-crystalline (001) n-type InP substrates were irradiated with 100 MeV $^{56}\text{Fe}^{7+}$ ions at fluences ranging from 5×10^{12} , 5×10^{13} and $1 \times 10^{14} \text{ cm}^{-2}$ at room temperature, using the 15 UD Pelletron facilities at Inter University Accelerator Centre (IUAC), New Delhi. Ion beam scanning was used to irradiate the whole sample surface in a uniform way. In order to prevent the heating during irradiation, the beam current was held at 3–4 pA (particle nano-ampere) and the sample was mounted on the copper target ladder with silver paste giving a good thermal conduction between them.

The ultraviolet-visible-near infrared measurements of the non-irradiated and samples irradiated with 100 MeV $^{56}\text{Fe}^{7+}$ ions were performed using a Shimadzu UV-3600 UV-VIS-NIR spectrophotometer in transmittance and reflectance mode. The Raman scattering measurements were performed at room temperature on the LabRAM HR Raman spectrometer using the 514.5 nm line of an argon ion laser in the back scattering geometry. Fourier transform infrared absorption and reflection spectra for non-irradiated and irradiated samples were recorded in the spectral region $6000\text{--}400 \text{ cm}^{-1}$ using the Fourier transforms infrared spectrometer (Jasco FTIR-610). The far infrared Fourier transform reflection spectra were recorded on NICOLET MEGANA – 550 in the spectral range $400\text{--}50 \text{ cm}^{-1}$.

In order to perform electrical measurements on Schottky barrier diode on n-InP, it is highly desirable to deposit suitable ohmic contact metals/alloys over the top of the sample. For making ohmic contact on n-InP, the gold (Au) metal is chosen (8, 9). Before depositing Au on n-InP, the sample is properly cleaned and etched for removal of trichloroethylene (TCE) solvent for 10 minutes. It is then immersed in 1 % Hydrofluoric (HF) acid for 1 minute in order to remove native oxide layers from the surface of n-InP. The sample is then rinsed in deionised water for 5 minutes. After that it is immediately transferred to a diffusion pump operated (having liquid nitrogen trap) high vacuum deposition chamber. The Au is deposited over the top of n-InP by thermal evaporation method. The base pressure of the chamber is about 10^{-6} mbar. During evaporation the thickness of the Au is monitored using quartz crystal monitor. The typical thickness of the Au contacts is 100 nm. The ohmic contacts are tested by current-voltage (I-V) measurements and they exhibit low contact resistance. For current voltage measurement, unit consist of Aplab7112 regulated dc power supply (30 V DC, 2 A Max), PLA DM-9 multimeter for voltage and current measurement. Current Voltage measurement is done on non - irradiated, 5×10^{10} , $1 \times 10^{11} \text{ cm}^{-2}$ samples at room temperature. The capacitance – voltage (C-V) measurements were performed using LCR meter HP 4284A (20Hz to 1MHz). The capacitance meter can measure the capacitance in the ranges of 10 pF to 9.99999 F. The capacitance – voltage measurements were carried out for non - irradiated, 5×10^{10} and $1 \times 10^{11} \text{ cm}^{-2}$ at the frequency of 1 MHz at room temperature.

Result and Discussion:

Ultraviolet-Visible-Near Infrared Studies:

Ultraviolet-visible-near infrared (UV-VIS-NIR) reflectance and transmittance spectra of non-irradiated indium phosphide and the samples irradiated with 100 MeV $^{56}\text{Fe}^{7+}$ ions for different ion fluences of 5×10^{12} , 5×10^{13} and $1 \times 10^{14} \text{ ions cm}^{-2}$ were recorded in the spectral region 200 nm to 1600 nm. Figure-1 shows the UV-VIS-NIR transmittance spectra of the non-irradiated sample and samples irradiated for fluence of 5×10^{12} , 5×10^{13} and $1 \times 10^{14} \text{ ions cm}^{-2}$.

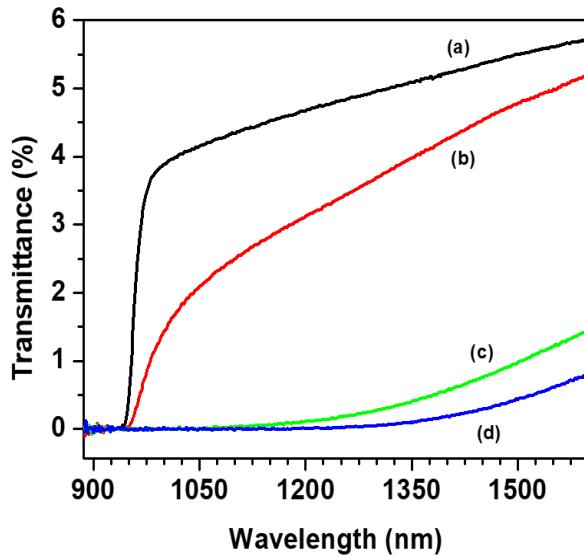


Fig. – 1: Variation of transmission intensity as a function of wavelength of indium phosphide samples; (a) non-irradiated and irradiated with 100 MeV $^{56}\text{Fe}^{+7}$ ions for fluence of (b) 5×10^{12} , (c) 5×10^{13} and (d) 1×10^{14} ions cm^{-2} .

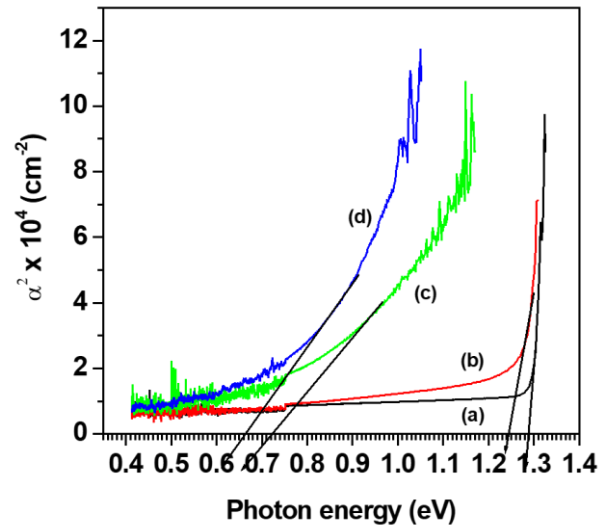


Fig. – 2: α^2 versus photon energy curve of indium phosphide samples irradiated with 100 MeV $^{56}\text{Fe}^{+7}$ ions: (a) non-irradiated, (b) 5×10^{12} (c) 5×10^{13} and (d) 1×10^{14} ions cm^{-2} .

The spectra of irradiated in figure -1 indium phosphide shown in exhibit two effects:

- ❖ Transmission intensity tends to decrease.
- ❖ Absorption edge shift towards the higher wavelength.

To estimate the band gap energy, α^2 versus photon energy ($h\nu$) graphs for non-irradiated and samples irradiated for various ion fluences were plotted (Figure - 2). The straight-line portion extrapolated at $\alpha^2 = 0$ gives the energy band gap. The values of energy band gap of the samples irradiated for fluence of 5×10^{12} , 5×10^{13} and 1×10^{14} ion cm^{-2} were found to be 1.25, 0.72 and 0.66 eV respectively, whereas corresponding estimate for the non-irradiated InP was 1.34 eV. The decrease in energy band gap is due to the presence of defects and disorder in the irradiated samples.

Fourier Transform Infrared Transmission Spectroscopy:

The Fourier transform infrared transmission spectra of indium phosphide samples irradiated with 100 MeV $^{56}\text{Fe}^{+7}$ ions for ion fluences of 5×10^{12} , 5×10^{13} and 1×10^{14} ions cm^{-2} were recorded in the spectral region 6000 cm^{-1} to 400 cm^{-1} . Figure -1 shows the transmission spectra of indium phosphide irradiated with various ion fluence. The transmittance spectrum of non-irradiated indium phosphide is also shown in the Figure - 3 for comparison. It can be seen from this figure that the transmission intensity of the samples irradiated for various ion fluences decreases with increase in ion fluence.

Optical density ($\alpha.d$) for the indium phosphide samples irradiated with various ion fluence were calculated from the transmission spectra (Figure 1) in the photon energy range 0.2 eV to 0.75 eV using the following equation (9)

$$\text{Optical density} = \ln \left[-(1 - R)^2 + \frac{\{(1 - R)^4 + 4T^2R^2\}^{\frac{1}{2}}}{2TR^2} \right]$$

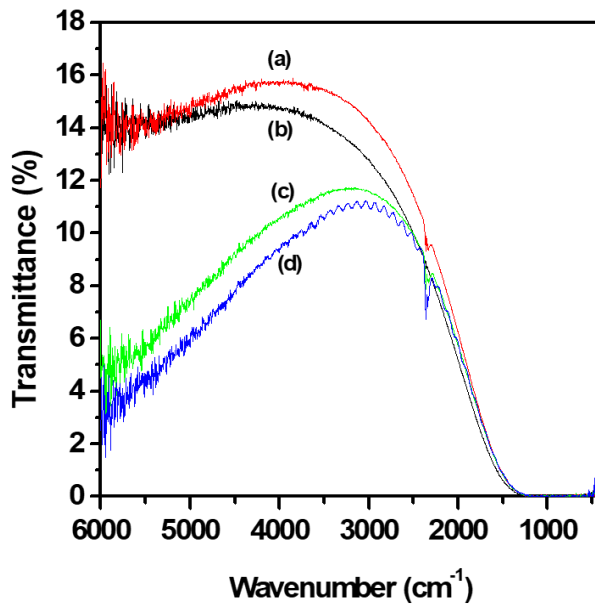


Fig. – 3: Fourier transform infrared transmission spectra of Indium phosphide samples; (a) non-irradiated and irradiated with 100 MeV $^{56}\text{Fe}^{+7}$ ions for fluence of (b) 5×10^{12} , (c) 5×10^{13} and (d) 1×10^{14} ions cm^{-2} .

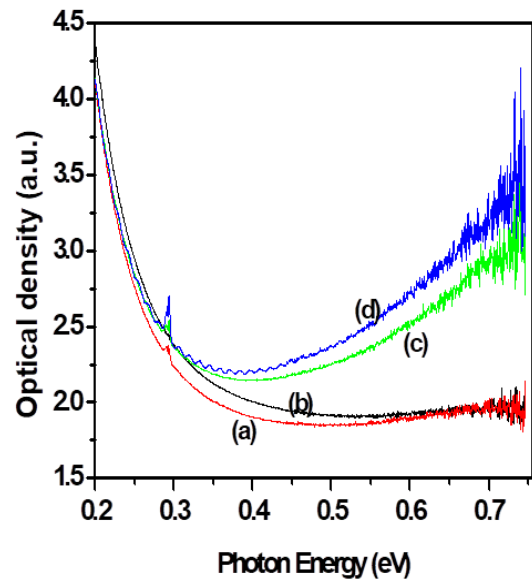


Fig. – 4: Optical density v/s photon energy of Indium phosphide samples; (a) non-irradiated and irradiated with 100 MeV $^{56}\text{Fe}^{+7}$ ions for fluence of (b) 5×10^{12} , (c) 5×10^{13} and (d) 1×10^{14} ions cm^{-2} .

Optical density

Figure – 4 shows the optical density versus photon energy plots for the non-irradiated and samples irradiated for various ion fluences. It is evident from the Figure that the optical density of non-irradiated and irradiated samples decreases in the photon energy region 0.2 eV to 0.75 eV. The increase in the optical density with ion fluence may be due to increase in the amount of disorder and defect concentrations in indium phosphide.

Defect Density

Ion irradiation induced defect density (N_s) in the irradiated samples was estimated using the following relation [9],

$$N_s = n \left[\frac{m_e c}{2\pi^2 e^2 \hbar} \right] \left[\frac{3}{n^2 + 2} \right]^2 \frac{1}{f} \int \alpha (\text{excess}) dE$$

where $\int \alpha (\text{excess}) dE$ is the difference in the areas under the optical density versus photon energy curves of non-irradiated and samples irradiated with various ion fluence, n is the refractive index of indium phosphide, c is the speed of light, e is the electronic charge and f is the oscillator strength and has been assumed to be one.

The defect density of the samples irradiated for ion fluences 5×10^{12} , 5×10^{13} and 1×10^{14} ions cm^{-2} was found to be 3.17×10^{15} , 2.0×10^{16} and 2.7×10^{16} cm^{-3} , respectively.

Annealing Effect

To study annealing effect, the sample irradiated with 5×10^{13} ions cm^{-2} was annealed at 200°C for 3 minutes. Variation of optical density with respect to photon energy for non-irradiated, as irradiated and annealed samples is presented in figure - 5. After annealing, estimated defect density was found to be $1.4 \times 10^{16} \text{ cm}^{-3}$ whereas the value of defect density for as irradiated sample was $2.0 \times 10^{16} \text{ cm}^{-3}$. The decrease in the defect density is due to reduction of the defect and disorder present in the irradiated samples.

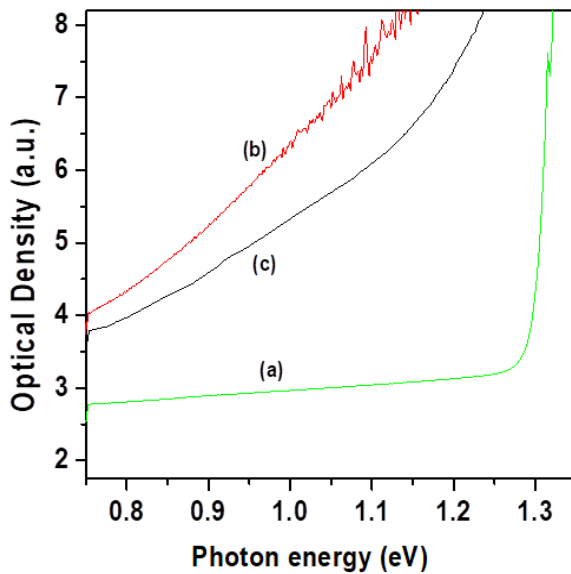


Fig. - 5: Annealing behavior of the InP sample irradiated for fluence of 5×10^{13} ions cm^{-2} at 100 MeV $^{56}\text{Fe}^{+7}$ ions: (a) non-irradiated, (b) as irradiated and (c) annealed at 200°C

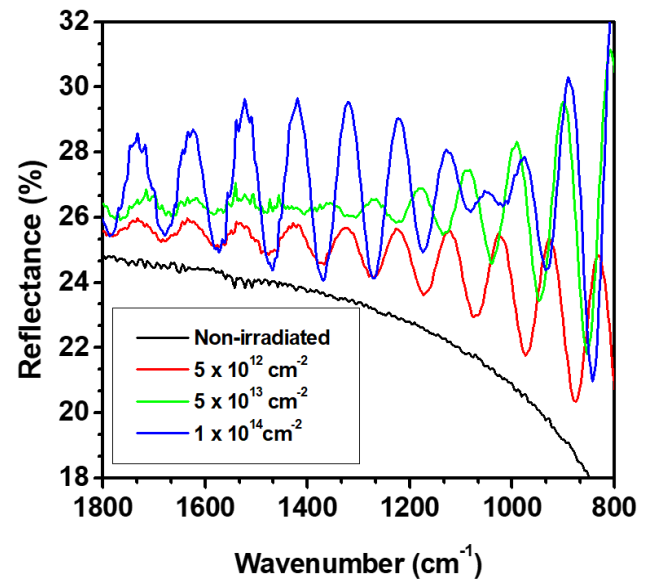


Fig. - 6: Fourier transform infrared reflectance spectra of non-irradiated and Indium phosphide samples irradiated with 100 MeV $^{56}\text{Fe}^{+7}$ ions for various fluence.

Fourier Transform Infrared Reflection Spectroscopy

Figure - 6 shows the Fourier transform reflectance spectra of non-irradiated indium phosphide and the samples irradiated for fluences of 5×10^{12} , 5×10^{13} and 1×10^{14} ions cm^{-2} . It is seen from the figure that the spectrum recorded for various ion fluence exhibits interference fringes in the spectral region 1600 cm^{-1} to 800 cm^{-1} , indicating that the refractive index of irradiated layer differs from the underlying indium phosphide substrate. The thickness of the irradiated layer was estimated from the fringe shift using the following equation [10],

$$d = 1/2n(\nu_1 - \nu_2)$$

Where d is the thickness of irradiated layer, n is refractive index and ν_1 , ν_2 are the wavenumber of successive maxima or minima of the interference fringes. The thickness of the irradiated layer for the fluence of 5×10^{12} , 5×10^{13} and 1×10^{14} ions cm^{-2} were found to be 16.13, 17.74 and 19.71 μm respectively which is comparable to the projected range (16.24 μm) of 100 MeV $^{56}\text{Fe}^{+7}$ ion in the InP. For fluence $1 \times 10^{14} \text{ cm}^{-2}$, more pronounced interference fringes appeared. It is evident from the figure - 6 that the increase in ion fluence increases their amplitude and position of the maxima and minima shifts.

Raman Scattering Measurements

The Raman scattering spectra of non-irradiated and the samples irradiated with 100 MeV $^{56}\text{Fe}^{+7}$ ions were shown in figure - 7. The first-order Raman spectra exhibits two peaks:

- ❖ one strong peak at 344.28 cm^{-1}
- ❖ other weak peak at 305.07 cm^{-1} , which correspond to characteristic LO and TO Raman modes of crystalline indium phosphide respectively.

It is important to mention that only LO mode is allowed for scattering by (100) face. However, in our studies, a small peak due to TO mode is also observed. This may be due to slight substrate misorientation.

- ❖ The spectra obtained from the samples irradiated with various ion fluences showed the decrease in the intensity of Raman peak with respect to ion fluence.
- ❖ The peak position also shifted towards the lower wave number due to presence of stress in the irradiated samples. The decrease in the intensity indicates the appearance of defects after ion irradiation.

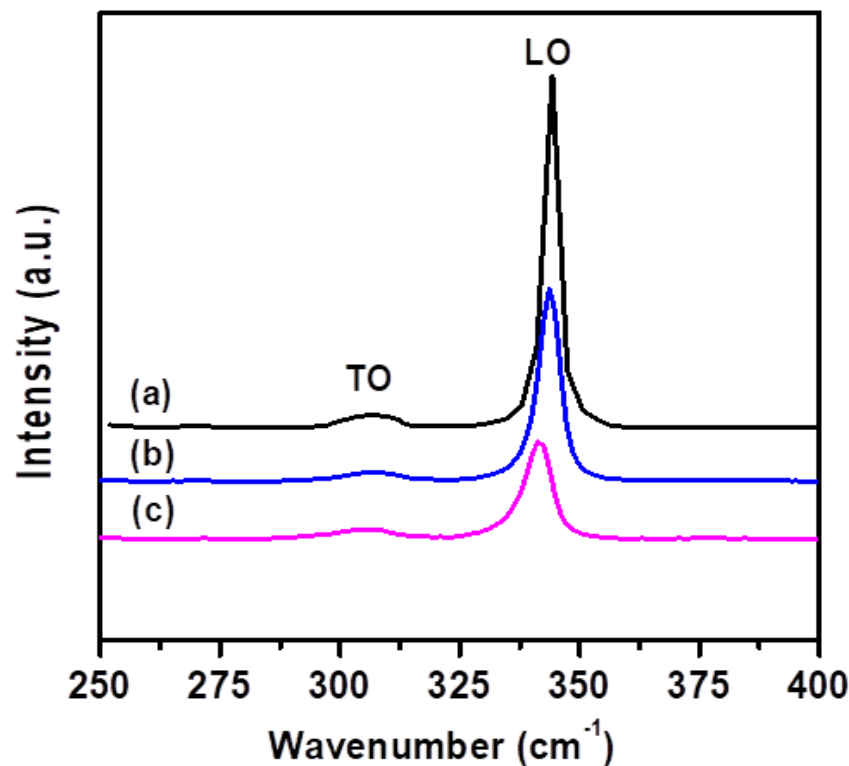


Fig. – 7: First-order optical Raman spectra of indium phosphide samples; (a) non-irradiated and irradiated with 100 MeV $^{56}\text{Fe}^{+7}$ ions for fluence (b) 5×10^{13} and (c) 1×10^{14} ions cm^{-2} .

Current – Voltage (I – V) Measurements

Schottky barrier diode on n-InP is fabricated by deposition of metal (Au) electrodes of 1 mm diameter on the implanted side and ohmic contact on the reverse side of the samples using the vacuum thin film deposition technique. The current – voltage (I-V) measurements were carried out at room temperature. I–V characteristic of the Au/InP Schottky barrier diode is shown in Figure - 8. I–V

characteristic gives a straight line only over that portion of the curve where $kT/q \ll V$ and $IR \ll V$. The straight-line portion of the plot yields reverse saturation current (I_s) by extrapolating it to $V = 0$. The ideality factor [11] for non-irradiated and various ion fluence was estimated using the following equations (11)

$$n = \frac{q}{kT} \frac{\partial V}{\partial(\ln I)}$$

where n is ideality factor, q is the electronic charge, k is the Boltzmann constant, T is the temperature, V is the applied voltage.

Barrier height for the fluence 5×10^{10} ions cm^{-2} and 1×10^{11} ions cm^{-2} were found to be 0.476 and 0.456 eV, respectively. Current voltage characteristic in forward bias condition shows that the current increases linearly in the voltage range 0-0.5 volt. Beyond this range, Schottky diode attains the saturation. However, the saturation decreases with the ion fluence. In the reverse bias, reverse saturation current is found to increase with ion fluence. The value of reverse saturation current for fluence 5×10^{10} and 1×10^{11} ions cm^{-2} were found to be 376.2 and 654.0 μA respectively whereas corresponding value for non-irradiated sample was 155.6 μA . Table – 1 shows the Value of the ideality factor, barrier height and reverse saturation current for non-irradiated and irradiated sample.

Table – 1: Parameter of 100 MeV $^{56}\text{Fe}^{+7}$ ions irradiated InP sample obtained from the $I - V$ characteristic

Fluence (Ion cm^{-2})	Ideality factor	Barrier Height (eV)	Reverse saturation current (μA)
Non irradiated	1.21	0.479	155.61
5×10^{10}	3.26	0.476	376.20
1×10^{11}	9.20	0.456	654.02

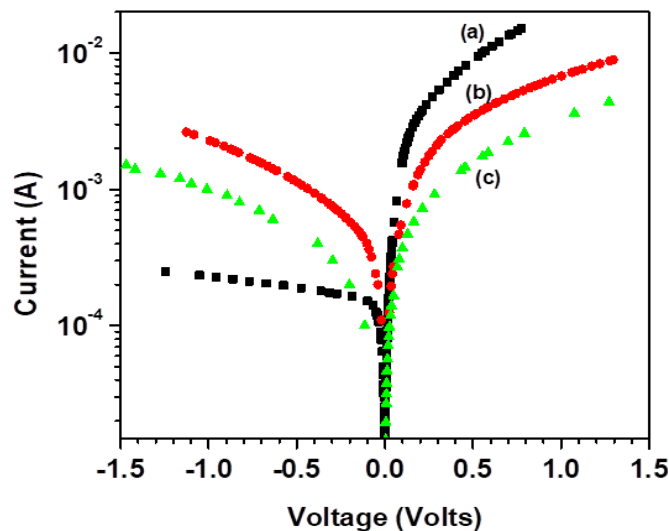


Fig. – 8: Voltage versus current plots of (a) non-irradiated indium phosphide and samples irradiated with 100 MeV $^{56}\text{Fe}^{+7}$ ions for fluence (b) 5×10^{10} and (c) 1×10^{11} ions cm^{-2}

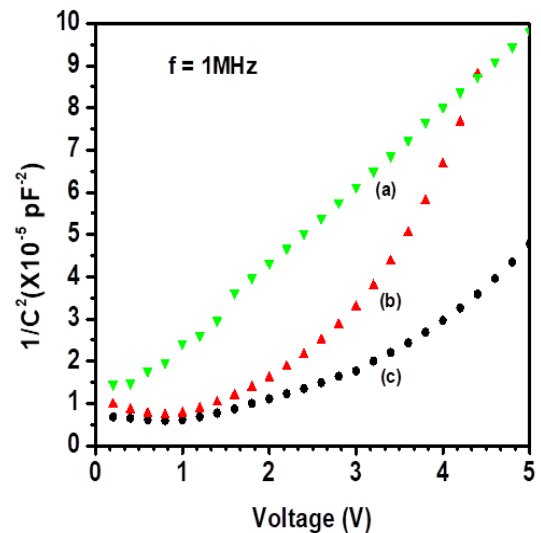


Fig. – 9: $1/C^2$ versus voltage plots of (a) non-irradiated indium phosphide and samples irradiated with 100 MeV $^{56}\text{Fe}^{+7}$ ions for ion fluences of (b) 5×10^{10} and (c) 1×10^{11} ions cm^{-2}

Capacitance – Voltage (C–V) Measurements

The capacitance-voltage (C-V) measurements were also carried out at room temperature for fluence 5×10^{10} and 1×10^{11} ions cm^{-2} . Figure - 9 represents the capacitance - voltage (C–V) characteristics of Au/InP Schottky barrier diode. Carrier concentration was estimated using following Equation (11)

$$N_D = \frac{2}{q\epsilon_s A^2 \left[d \left(\frac{1}{C^2} \right) / dV \right]}$$

Carrier concentration (N_D) was estimated as 1.02×10^{20} and 3.15×10^{19} cm^{-3} for fluence 5×10^{10} and 1×10^{11} ions cm^{-2} respectively. However corresponding estimate for the non-irradiated sample was 1.74×10^{20} cm^{-3} .

Conclusion:

- Raman scattering spectroscopy measurements were carried out to understand disorders and related defects induced in the surface region of the crystalline indium phosphide due to the swift iron ion irradiation.
- The appearance of interference fringes with increasing amplitude and shift in the maxima and minima positions, in the Fourier transform reflectance spectra of irradiated samples showed the change in the refractive index of the irradiated layer due to presence of point defect or defect clusters in the sample.
- The decrease in the defect density is due to reduction of the defect and disorder present in the irradiated samples.
- The energy band gap of irradiated indium phosphide decreased very smoothly with increase in the ion fluence.
- The decrease in energy band gap is due to the presence of defects and disorder in the irradiated samples.

Conflict of Interest:

The authors declared that they have no conflict of interest.

References:

- [1] Humphreys, B.; O'Donnell, A. Compound Semiconductors, Institute of Physics Publishing Ltd, August 2003; Whitaker, T. Compound Semiconductors, Institute of Physics Publishing Ltd, January 2004.
- [2] Wesch, W.; Kamarou, A.; Wendler, E.; Klaumünzer, S. Nucl. Instrum. Methods B 2006, 242, 363–366.
- [3] Kamarou, A.; Wesch, W.; Wendler, E.; Klaumünzer, S. Nucl. Instrum. Methods B 2004, 225, 129–135.
- [4] Kamarou, A.; Wesch, W.; Wendler, E.; Undisz, A.; Rettenmayr, M. Phys. Rev. B 2006, 73, 184107-1–16.
- [5] Singh, J.P.; Singh, R.; Mishra, N.C.; Ganesan, V.; Kanjilal, D. J. Appl. Phys. 2001, 90, 5968–5972



- [6] Ciatto, G.; D'Acapito, F.; Fraboni, B.; Boscherini, F.; El Habra, N.; Cesca, T.; Gasparotto, A.; Moreira, E.C.; Priolo, F. Nucl. Instrum. Methods B 2003, 200, 100–104.
- [7] Gasparotto, A.; Fraboni, B.; Priolo, F.; Enrichi, F.; Mazzone, A.; Scamarcio, G.; Troccoli, M.; Mosca, R. Mater. Sci. Eng. B 2001, 80, 202–205.
- [8] S. K. Ghandhi, VLSI Fabrication Principles (John Wiley & Sons, 1994).
- [9] D. K. Schroder, Semiconductor Material & Device Characterization, 3rd edition (John Wiley & Sons).
- [10] E. Wendler and G. Peiter, *J. Appl. Phys.* 87 (2000) 7679.
- [11] Sandeep kumar, Y S katharria, Sugam Kumar and D kanjilal, *J of Appl. Phys.* 100 (2006) 113723.